

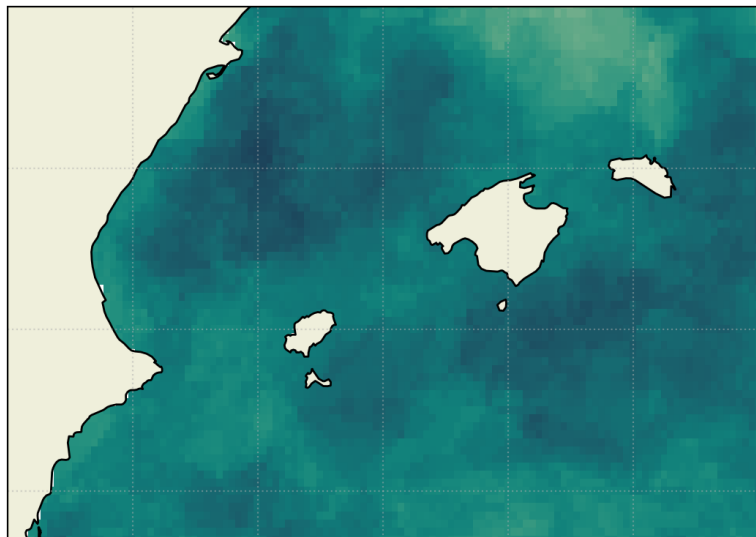
Internship Final Report - Master II Ocean Data Science

Marine heatwaves in the Balearic Islands region

Author: Arthur Gonnet, IMT Atlantique, arthur.gonnet@imt-atlantique.net

Under the supervision of: Mélanie Juza and Emma Reyes

Hosting institution: SOCIB-ICTS, Spain



April - September 2025

Abstract

In the context of global warming, marine heatwaves (MHWs) are increasing in frequency, intensity and duration. The Mediterranean Sea is being particularly affected by this phenomenon, and especially the Balearic Islands region, recognised as a biodiversity hotspot. This study proposes to analyse the spatio-temporal variability of surface and subsurface MHWs in this region. To this end, satellite observation-derived sea surface temperature (SST) records and a regional physical reanalysis have been used to investigate surface and subsurface MHWs for the periods 1982-2023 and 1987-2022, respectively. MHW calculations have been applied to those two datasets under a consolidated common methodology, considering four subregions. In line with other studies, this study shows that MHWs metrics exhibit strong spatial, vertical and temporal variations. Also, it highlights positive trends in annual MHW metrics at the surface, as well as in the subsurface. Furthermore, subsurface MHWs present weaker intensities but greater persistence than surface MHWs, with a maximum around 500 m depth. At the surface, a north/south contrast has been identified in the region, with stronger intensities in the northern area but longer-lasting events in the southern area. At depth, the Balearic Sea subregion has stronger persistence than the north-western Algerian subregion. These findings underline the need for sustained and continuous deep ocean monitoring to improve the detection and prediction of MHWs both at the surface and subsurface, in order to better assess their growing ecological risks.

Keywords

Marine heatwaves, Balearic Islands, surface and subsurface, long-term changes

Acknowledgments

I would like to thank my two supervisors, Mélanie Juza and Emma Reyes, for giving me the opportunity to join SOCIB and for dedicating their time to me throughout my internship.

I am also grateful to my colleagues and friends at SOCIB for their warm welcome and for all the time and discussions we shared during my internship.

Finally, I would like to thank the professors at IMT Atlantique, IUEM and ENSTA Bretagne for providing me with the necessary tools to conduct this study.

Table of Contents

1. Introduction.....	4
2. Data.....	6
2.1. Satellite-derived data.....	6
2.2. Model reanalysis data.....	6
3. Methods.....	6
3.1. Marine heatwaves detection.....	6
3.2. Annual metrics.....	7
3.3. Subregions considerations.....	8
3.4. Levels selection.....	9
3.5. Statistical analysis.....	9
4. Surface MHWs (REP).....	10
4.1 Spatio-temporal variability.....	10
4.2 Linear trends.....	13
4.3 Sensitivity to the period.....	13
4.4 Model assessment.....	14
5. Subsurface MHWs (MEDREA).....	15
5.1. Regional analysis.....	15
5.2. Subregional analysis.....	18
6. Drivers of specific MHW events.....	20
6.1. Atmospheric forcing.....	20
6.2. Anticyclonic eddies.....	21
6.3. Other vertical processes.....	22
7. Conclusion and perspectives.....	23
Appendices.....	31

1. Introduction

Global warming is driving profound transformations in the ocean, with extreme temperature events emerging as one of the most acute manifestations of climate change. More than 90% of the excess heat accumulated in the Earth system is stored in the ocean, resulting in significant warming of surface and subsurface layers (Cheng et al., 2024; Pan et al., 2025). The Mediterranean Sea, due to its semi-enclosed nature, limited volume, and intense anthropogenic pressures, is recognised as a climate change hotspot (Giorgi, 2006; Lionello and Scarascia, 2018). More precisely, its surface warming rate is more than three times faster than the global ocean over the past four decades. Since 1982, the Mediterranean Sea basin-averaged sea surface temperature (SST) has been warming at a mean rate of 0.41 ± 0.01 °C/decade over the period 1982-2023 (von Schuckman et al., 2024) and 0.44 ± 0.02 °C/decade over 1982-2024 (updated estimations from Juza and Tintoré, 2020, 2021) compared with the global ocean warming trend, which has been estimated at 0.13 ± 0.01 °C/decade over 1982-2023 (von Schuckman et al., 2024).

In this context of intense ocean warming, marine heatwaves (MHWs), defined as prolonged periods of anomalously warm ocean temperature (Hobday et al., 2016), are becoming more frequent, more intense and longer-lasting worldwide (Frölicher et al., 2018; Oliver et al., 2018) and in the Mediterranean Sea (Juza et al., 2022; Dayan et al., 2023; Martínez et al., 2023). The study of these events has emerged

as a growing area of interest due to their wide impacts on the marine ecosystems. They include widespread coral and gorgonian bleaching, seagrass meadows declining, mass mortality events of marine organisms or location shifts of distribution (Garrabou et al., 2022; Wernberg et al., 2013; Holbrook et al., 2020; Guerrero-Meseguer et al., 2017). The resulting marine life deterioration has impacts on economic sectors goods, such as marine living resources and tourism (Smith et al., 2021). Human health can also be affected by extreme event intensification through infectious disease, harmful algal blooms, proliferation of jellyfish or lack of food (United Nations Environment Programme, 2021). Finally, bringing more heat and moisture to the atmosphere, warm waters can contribute to the intensification of extreme events such as storms with heavy rainfalls that can cause flooding, beach loss or infrastructure destruction (Mitchell et al., 2006).

This study focuses on the Balearic Islands region, located in the western Mediterranean, which is particularly vulnerable. It is a well-known biodiversity hotspot (Coll et al., 2010) exposed to intense anthropogenic pressures and severely affected by climate change (Pisano et al., 2020; Garrabou et al., 2022; Juza et al., 2022, 2024). This region is also part of the Cetacean Migration Corridor Specially Protected Area of Mediterranean Importance (Cardona et al., 2025), making its conservation highly relevant. Moreover, this region has been selected as a pilot area to develop and implement a Digital Twin of the Ocean (DTO) in the

western Mediterranean Sea (operated by SOCIB; Reyes et al., 2024), aiming to integrate multi-platform observations and models to improve monitoring and prediction of ocean indicators and climate-driven hazards such as MHWs. Understanding how MHWs manifest in this area, both at the surface and in the subsurface, is therefore crucial to anticipate ecological risks and to strengthen regional climate adaptation strategies.

To date, numerous studies have characterised MHWs at the surface thanks to the daily and continuous monitoring of SST by satellites since 1982. These long observed time series have enabled analysis at a global scale (Holbrook et al., 2019; Oliver et al., 2018; Sen Gupta et al., 2020), at basin scale (e.g. Mediterranean Sea) (Martínez et al., 2023; Juza et al., 2022, 2024; Simon et al., 2023; Pastor and Khodayar, 2023; Rosselló et al., 2023) or at regional scales, as in the Balearic Sea (Fernández-Álvarez et al., 2025). However, most of these efforts have focused on the surface ocean, leaving the subsurface dynamics less explored due to the sparsity of long-term observational records. Thanks to the multi-platform observing systems and improved models, the study of the three-dimensional structure of MHWs is emerging but still limited (Capotondi et al., 2024; Juza et al., 2022). Recent studies have highlighted that subsurface MHWs may be equally or even more persistent than surface events (Zhang et al., 2023; Dayan et al., 2023; Juza et al., 2022). In the Mediterranean, subsurface assessments reveal that MHWs penetrate below 200 m, with distinct temporal and spatial patterns (Dayan et

al., 2023; Juza et al., 2022). Focus on the comparison of MHW at the ocean surface and bottom has been carried out in Amaya et al. (2023a) along the continental shelves of North America and Fernández-Barba et al. (2024) along the Spanish coast. In the Balearic Islands region, the coastal and vertical variability of MHWs remains poorly explored, despite evidence that mesoscale and submesoscale processes, such as eddies, upwelling, and stratification, strongly modulate their occurrence and intensity in nearshore waters (Schaeffer and Roughan, 2017; Juza et al., 2022; Fernández-Barba et al., 2024). In this context, the present study aims to investigate surface and subsurface MHWs around the Balearic Islands by combining satellite observations and a regional model reanalysis, focusing on their spatio-temporal variability across coastal and deeper zones.

This report is structured as follows: First, the satellite and model data used in this study are described in **Section 2**. **Section 3** describes the methods used for the MHW calculation and characterisation, introduces the subregional approach and selected depth levels for analysis, and presents the methodology applied for statistics. Then, the results for surface and subsurface MHWs, derived from satellite observations and the model, are described and discussed in **Sections 4** and **5**, respectively. Also, specific MHW events are addressed in **Section 6**. Finally, **Section 7** summarises the main conclusions of the study and provides perspectives.

2. Data

In this study, two datasets, provided by Copernicus Marine Service (<https://marine.copernicus.eu/>), are used. The satellite-derived SST record (herein referred to as REP; **Section 2.1**) is used for the analysis of MHWs at the surface, while a regional physical reanalysis (herein referred to as MEDREA; **Section 2.2**) is used for studying surface and subsurface MHWs.

2.1. Satellite-derived data

REP consists of daily (at nighttime), high-resolution, reprocessed gap-free foundation sea surface temperature (SST) (namely, the temperature free, or nearly-free, of any diurnal cycle) L4 (Level 4) maps¹ covering the Mediterranean Sea and the adjacent North Atlantic box (Pisano et al., 2016; Embury et al., 2024). REP has a horizontal grid resolution of $1/20^\circ \times 1/20^\circ$ (ca. 5-6 km) and extends from 1982 to present. In this study, the REP product is analysed over the period 1982-2023.

2.2. Model reanalysis data

MEDREA consists of a daily, high-resolution, four-dimensional physical reanalysis² covering the Mediterranean Sea (Escudier et al., 2020). It is generated by a numerical system composed of a hydrodynamic model,

supplied by the Nucleus for European Modelling of the Ocean (NEMO) and a variational data assimilation scheme (OceanVAR) for temperature and salinity vertical profiles and satellite sea level anomaly along-track data. MEDREA has a horizontal grid resolution of $1/24^\circ \times 1/24^\circ$ (ca. 4-5 km), 141 unevenly spaced vertical levels from the surface up to 5754 m depth, and extends from 1987 to May 2023 (at the time of writing). In this study, the MEDREA product is analysed over the period 1987-2022.

3. Methods

3.1. Marine heatwaves detection

The detection of MHWs follows a consolidated common approach defined in Hobday et al. (2016). Thus, an anomalously warm water event is considered a MHW if the temperature exceeds for at least five consecutive days the 90th percentile based on a historical baseline period. Two successive MHWs with a break of two days or less are considered a single continuous event. The daily mean and 90th percentile climatology are smoothed using a 30-day moving window. Each dataset, REP and MEDREA, uses its own climatology to detect MHWs.

For each MHW day (a day meeting MHW conditions), the MHW intensity, category and severity are defined. The MHW intensity refers to the daily temperature anomaly (difference between the observed temperature and the mean climatology). The MHW category is defined as in Hobday et al. (2018), each category having as

¹ https://data.marine.copernicus.eu/product/SST_MED_SST_L4 REP_OBSERVATIONS_0_021/ description (Accessed on 30 August 2025)

² https://data.marine.copernicus.eu/product/MEDSEA_MULTIYEAR_PHY_006_004/ description (Accessed on 30 August 2025)

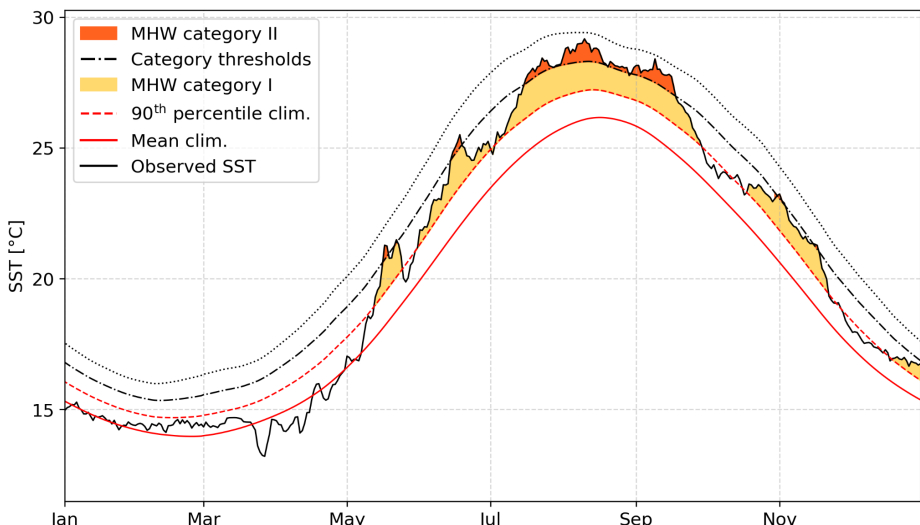


Figure 2 | Daily SST from REP averaged over the Balearic Islands region in 2022 (black line). Mean and 90th percentile climatology with respect to the period 1987-2021 (red solid and dashed lines, respectively) are shown. Multiples of delta (90th percentile minus mean climatology; black dashed lines) describe different categories of MHWs, being in yellow and orange for moderate (category I) and strong (category II) MHW events, respectively.

threshold a multiple of the 90th percentile climatology relative to the mean climatology (delta), as displayed in **Figure 2**. The MHW severity is defined as in Sen Gupta et al. (2020), representing a continuous counterpart to the discrete category metric. It consists of the ratio between the MHW intensity and delta.

All along this study, the climatological baseline period is 1987-2021, being chosen specifically for this study as no common reference period is used in the literature. This period lasts more than 30 years as recommended by Hobday et al., 2016. This choice is also motivated by the period starting with the earliest data available in both datasets, and excluding 2022 to be able to compare it to the prior years' climatology, as it has been an exceptional year in western Mediter-

ranean Sea water temperatures (Juza et al., 2024).

3.2. Annual metrics

Annual MHW metrics have been defined to estimate long-term changes in MHW characteristics over the last four decades. Given the MHW metrics defined above, annual metrics are derived on a yearly basis as defined in **Table 1**.

In this study, the Python package developed and made publicly available by Eric C. J. Oliver and referenced in Hobday et al. (2016) has been adapted and applied to perform MHW calculation. The codes have been made available in open access at <https://github.com/arthur-gonnet/balearic-mhws-study>. Details of the changes made to the original code can be found in GitHub commit “*Modifications to the marineHeatWaves*

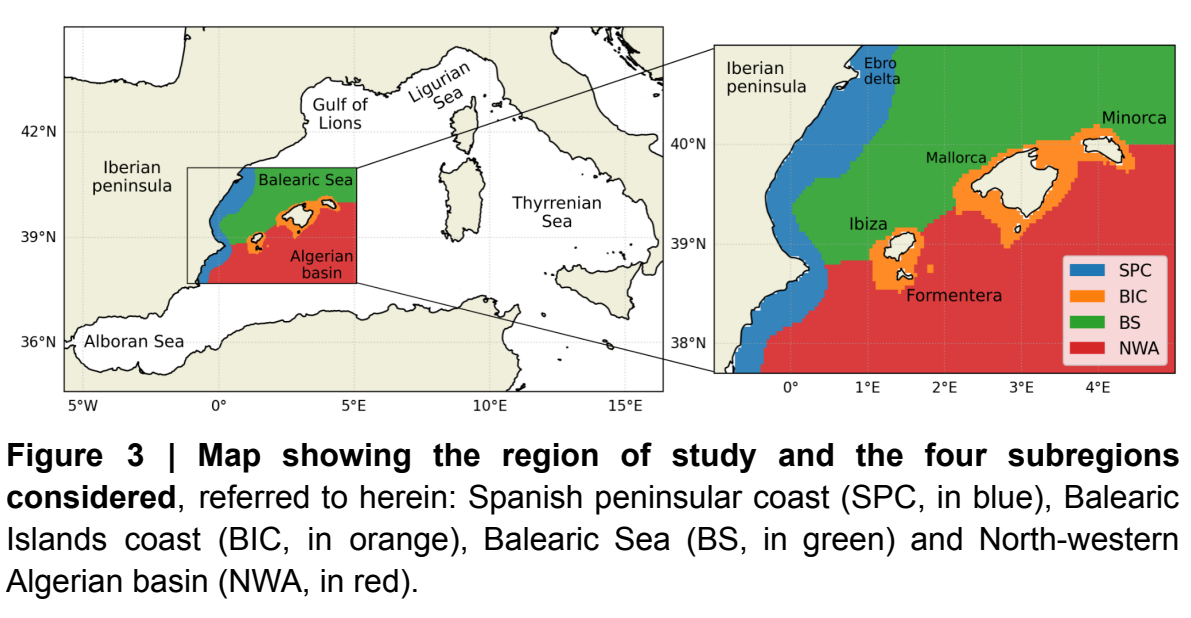
Table 1 | Annual metrics studied here to characterise MHWs.

Annual metric	Definition	Unit
Total days	Number of MHW days	days
Mean duration	Average duration of MHW events	days
Cumulative intensity	Sum of MHW intensity over all MHW days	°C·days
Maximum intensity	Maximum MHW intensity observed on a MHW day	°C
Mean intensity	Average MHW intensity over all MHW days	°C
Mean severity	Average MHW severity over all MHW days	No unit

module". They include the addition of the mean severity metric and the alteration of the mean intensity annual metric to fit the definition used here (being a mean over MHW days rather than being over MHW events). Another modification concerns an unexpected behaviour that occurred with the total days annual metric, occasionally exceeding 366 days. Indeed, when a MHW event overlapped over two years, it was only considered for the year it began in (for example, with a 500-day lasting event starting in 2010, total days will be 500 days in 2010 alone). The found solution to overcome this concern is to cut events in two between 31st December and 1st January, to account only for what happened in the given year. This solution introduces a new bias as it may reduce the duration of MHW events when cutting them in two, affecting the mean duration metric.

3.3. Subregions considerations

The region of study is centred around the Balearic Islands, as shown in **Figure 3**. An interesting feature of this region is the diversity of dynamics at play, which motivated its subdivision into four subregions in order to capture potential differences in MHW characteristics. A primary distinction was made between coastal and deeper areas, as the coastal zone has higher ecosystem vulnerability and is subject to stronger human pressure (Juza et al., 2024; Garrabou et al., 2022). The limit of the coastal area has been chosen as the 200 m isobath, corresponding to the continental shelf break, consistent with the United Nations Convention on the Law of the Sea definition. Within the coastal domain, two subregions, the Spanish peninsular coast (SPC) and the Balearic Islands coast (BIC), are separated because they have different coastal ocean dynamics and land influences (e.g. river inputs).



Finally, the deeper area is divided into the Balearic Sea (BS) and the North-western Algerian basin (NWA), due to the different circulations they are subject to. The northern part (BS) is strongly influenced by the dynamics of the Gulf of Lions, through the Northern Current, which flows southwards along the continental coast and can bifurcate eastward along the northern shelf of the Balearic Islands, joining the Balearic Current. For its part, the southern part (NWA) is influenced by the Algerian current (Pinot et al., 1995; Millot, 1999). The separation of those two subregions is defined by the channels between the Balearic Islands, since they act as natural barriers that modulate the circulation and water mass exchange between these two subregions at depth. This subdivision of the study area, therefore, allows a more detailed assessment of spatial heterogeneity in MHW occurrence and intensity, taking into account both bathymetric constraints and regional circulation features.

3.4. Levels selection

In order to represent relatively detailed distributions of MHW statistics over the water column, 10 depth levels have been selected from MEDREA dataset. Those levels have been selected based on the different dynamics at play over the water column. The first 150 m, being the surface waters, are directly influenced by atmospheric forcing, as well as being part of the euphotic zone, where primary production is maximised (Lavigne et al., 2015). Below, in the 150-700 m layer, are the intermediate waters (Millot, 1999), showing a high change in Ocean Heat Content (OHC) in the world ocean over the last 50 years (Levitus et al., 2005). Finally, deep waters are considered to be located below 700 m. The 2000 m level has been chosen as the deepest level of this study, as only a restrained portion of the region has deeper bathymetry. Afterwards, intermediate levels have been selected between these key levels. In this report, the approached values of the MEDREA level depths will be used, as round

values of depth are not present in the model. Thus, the levels selected are: 1, 51, 98, 153, 203, 493, 702, 1005, 1487 and 2001 m.

3.5. Statistical analysis

Within this study, classical statistics have been used to describe time series: mean, standard deviation (STD) and trends. For **Table 2** and **Figures 6** and **9**, when computing the mean over the region and the period, the spatial average is applied before the temporal average. To assess the significance of the trends in time series, a modified Mann-Kendall test is applied. This test accounts for autocorrelation in time series (Hamed and Ramachandra Rao,

1998; Wang et al., 2020). It has recently been used in Dayan et al. (2023). To compute trend slopes, a Theil-Sen estimator is used, being a non-parametric method, robust to outliers (Helsel et al., 2020).

4. Surface MHWs (REP)

In this section, surface MHWs are studied using the observation REP product over the period 1982-2023. Means and trends of annual metrics are also studied over the period 1987-2022 to be compared to the MEDREA model in order to evaluate its reliability at the surface. The climatological baseline period remains 1987-2021.

Table 2 | Mean, standard deviation (STD), trend of the annual metrics derived from REP and MEDREA, averaged over the whole region, for the periods 1982-2023 and 1987-2022. Trends are given per decade.

Annual metric	Statistic	REP (1982-2023)	REP (1987-2022)	MEDREA (1987-2022)
Total days [days]	Mean ± STD	24 ± 37	24 ± 32	31 ± 38
	Trend	8.5	8.4	12.3
Mean duration [days]	Mean ± STD	10.5 ± 5.5	10.4 ± 5.3	12.7 ± 7.4
	Trend	1.07	0.98	Not significant
Cumulative intensity [°C·days]	Mean ± STD	45 ± 77	44 ± 69	51 ± 75
	Trend	15.0	15.0	19.9
Maximum intensity [°C]	Mean ± STD	2.28 ± 0.62	2.31 ± 0.57	2.07 ± 0.64
	Trend	0.30	0.28	0.34
Mean intensity [°C]	Mean ± STD	1.65 ± 0.27	1.66 ± 0.26	1.49 ± 0.32
	Trend	0.12	0.11	0.12
Mean severity	Mean ± STD	1.35 ± 0.12	1.36 ± 0.12	1.33 ± 0.14
	Trend	0.05	0.03	0.07

4.1 Spatio-temporal variability

In the Balearic Islands region, as derived from the satellite-observed SST, the annual MHW metrics averaged over both the region and the period 1982-2023 have values of 24 days, 10.5 days, 45 °C·days, 2.28 °C, 1.65 °C and 1.35 for total days, mean duration, cumulative, maximum and mean intensity and mean severity, respectively, as shown in **Table 2**.

The maps of the period-averaged annual metrics over 1982-2023 (**Fig. 4a-f**) show spatial variability over the region of study with values ranging from 20 to 28 days, from 9.1 to 16.0 days and from 37 to 59 °C·days for total days, mean duration and cumulative intensity, respectively (**Fig. 4a-c**). Maximum and mean intensities and mean severity range from 1.96 to 3.22 °C, from 1.46 to 2.19 °C and from 1.31 to 1.51, respectively (**Fig. 4d-f**). For the intensity-related metrics, there is a clear north-south contrast, with higher values in the northern part (SPC and BS) (**Fig. 4c-e**). For total days, mean duration and mean severity, no clear pattern emerges in the maps (**Fig. 4a-b,f**). These results are also reflected in **Figure 5**, which shows the evolution and period-averaged value of the four subregional-averaged annual metrics from 1982 to 2023. Again, the north-south difference stands out in the intensity-related metrics, with higher period-averaged values in the northern part (SPC and BS) than in the southern part (BIC and NWA). Period-averaged cumulative, maximum and mean intensities have values of 48 °C·days, 2.39 °C and 1.72 °C, respectively, for BS and of 43

°C·days, 2.18 °C and 1.58 °C, respectively, for NWA (**Fig. 5c-e**). Also, this figure shows some differences between the coastal and the open waters. In particular, the highest mean values of persistence-related metrics are in the coastal area of the Balearic Islands (BIC) with values of 25 and 11 days for total days and mean duration, respectively (**Fig. 5a-b**).

As also shown in **Figure 5**, the spatial variability of the annual metrics is combined with its temporal variability. This temporal variability is reflected in the high values of STD, as reported in **Table 2**, reaching 37 days and 77 °C·days for total days and cumulative intensity, respectively, corresponding to 1.5 and 1.7 times their respective mean value over the period. Mean duration also exhibits relatively high interannual variability (STD = 5.5 days), whereas maximum intensity, mean intensity and mean severity show lower variability relative to their means (STD = 0.62 °C, 0.27 °C and 0.12, respectively). **Figure 5** provides a clear illustration of this variability, with both gradual and abrupt variations over time in the annual metrics. For instance, both MHW total days and cumulative intensity show a similar pattern with low values until the late 90s, with a pronounced acceleration from 2015 onwards and extreme peaks in recent years. The peaks in the time series exhibit extraordinary MHW active years.

The 8 years with the highest region-averaged total days at surface are: 2022, 2023, 2016, 2017, 2003, 2020, 2015 and 2011, with values of 165, 153, 81, 75, 61, 58, 51 and 47 days, respectively. Except for 2015, all

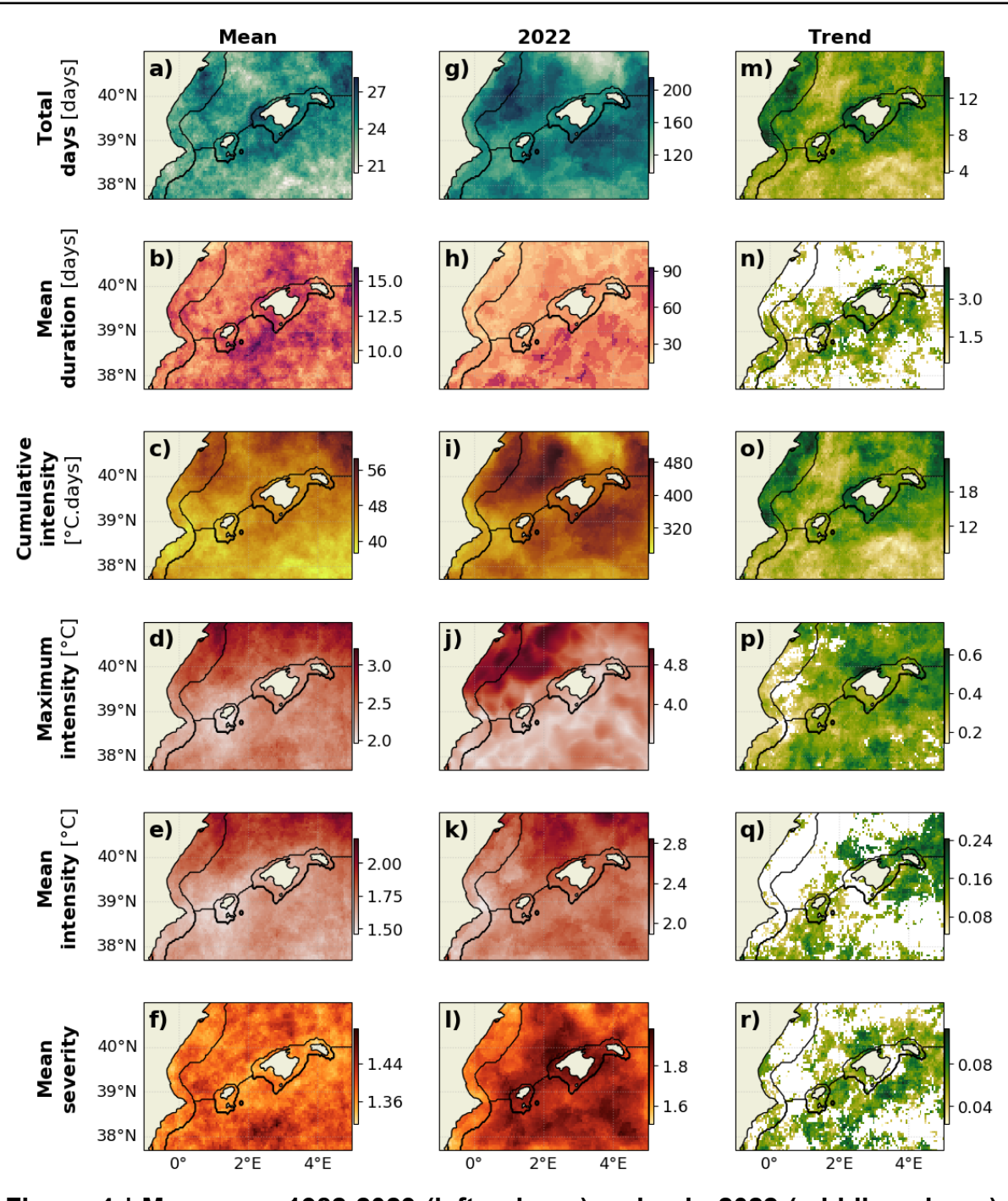


Figure 4 | Mean over 1982-2023 (left column), value in 2022 (middle column) and linear trend over 1982-2023 (right column) of the annual metrics derived from REP in the Balearic Islands region. Scales of colorbars for 2022 are higher than in the mean plots, since it was an anomalous year. Trends are given per decade. In the right column, non-significant trends are indicated in white. Black contours separate subregions.

those years correspond to local maxima in the time series (Fig. 5a). Furthermore, the high values in total days for these

years are not necessarily reflected in the other annual metrics. Indeed, the year 2016 recorded lows in terms of max-

imum and mean intensity (**Fig. 5d-e**). On the contrary, 2003 and 2022 specifically exhibit high values in all six annual metrics. For 2022, the region-averaged mean duration and cumulative intensity are 33.5 days and 381 °C·days, respectively (computations not shown). Region-averaged maximum and mean intensity and mean severity are 3.93 °C, 2.31 °C and 1.77, respectively. In the study period 1982-2023, it is the year with the highest regional average for every annual metric. Also, **Figure 4g-l** displays the spatial variability of annual metrics in 2022. Total days, mean duration and cumulative intensity reached local maximums of 215 days between Ibiza and the Ebro delta (**Fig. 4g**), 92 days under Ibiza (**Fig. 4h**) and 490 °C·days above Mallorca (**Fig. 4i**), respectively. Maximum and mean intensity and mean severity reached local maximums of 5.1 °C near the Ebro delta (**Fig. 4j**), 2.8 °C above Minorca (**Fig. 4k**) and 2.0 just west of Mallorca (**Fig. 4l**), respectively. Further investigation of specific surface MHW years will be addressed in **Section 6.1**.

Finally, **Figure 5** exhibits strong increases in annual metrics, in particular in recent years. These long-term variations will be analysed in the following section.

4.2 Linear trends

At the surface, MHWs are growing more persistent and more intense in the Balearic Islands region over the last four decades. Indeed, each annual MHW metric derived from REP shows a significant positive trend over 1982-2023 (**Table 2**). The number of total MHW

days, mean duration and the cumulative intensity have trends of 8.5 days/decade, 1.07 days/decade and 15.0 °C·days/decade, respectively. Maximum and mean intensity and mean severity have trends of 0.30 °C/decade, 0.12 °C/decade and 0.05 per decade, respectively. These trends point to future longer-lasting and thermally more stressful events.

The maps of long-term trends (**Figs. 4m-r**) confirm the widespread intensification of surface MHWs across the Balearic Islands region, but point to high spatial variability. Total days, cumulative intensity, and maximum intensity annual metrics highlight significant positive trends in most of the region, ranging from 3.8 to 14.3 days/decade, 7.4 to 23.8 °C·days/decade and 0.14 to 0.63 °C/decade, respectively (**Fig. 4m, o-p**). For mean duration, mean intensity, and mean severity, trends are also positive, ranging from 0.87 to 4.21 days/decade, 0.07 to 0.24 °C/decade and 0.03 to 0.11 per decade, respectively (**Fig. 4n, q-r**) with a marked fraction of locally non-significant trends. For total days, mean duration and cumulative intensity, the strongest increases are observed in coastal subregions, where the subregional-averaged trends are higher in SPC and BIC than in BS and NWA, with values of 10.2 and 9.3 days/decade for total days, 1.46 and 1.54 days/decade for mean duration and 16.2 and 15.4 °C·days/decade for cumulative intensity, respectively, compared with 8.7 and 7.3 days/decade for total days, 1.14 and 1.23 days/decade for mean duration and 15.1, 13.1 °C·days/decade for cumulative intensity, respectively (not shown). For maximum and mean

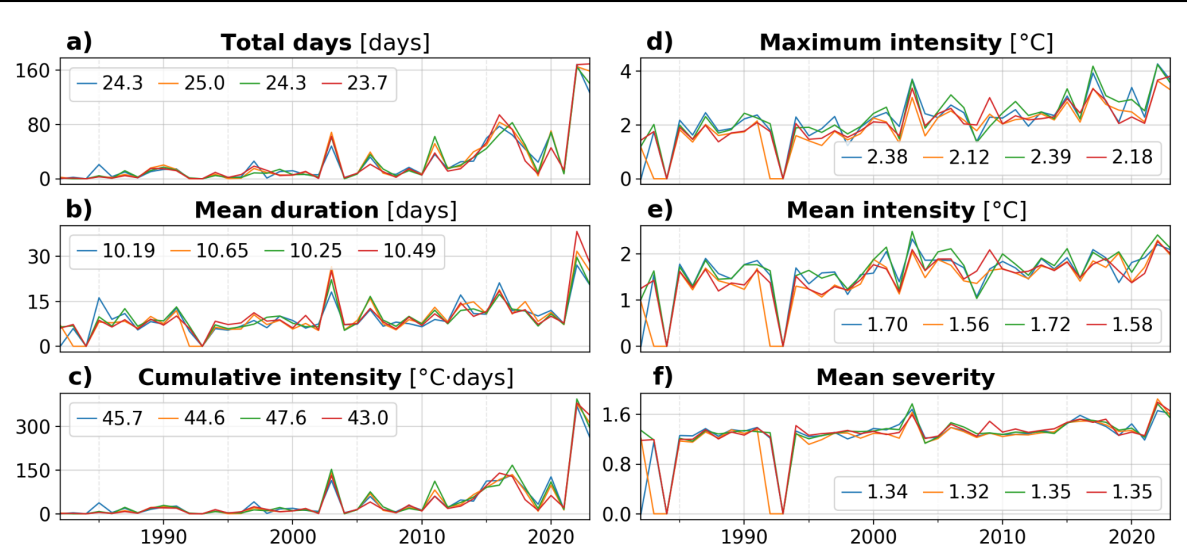


Figure 5 | Evolution of annual metrics derived from REP, averaged over the four subregions, over the period 1982-2023, at the surface. Subregions are shown: SPC in blue, BIC in orange, BS in green and NWA in red. Mean value for each subregion over the period is displayed in the legend.

intensity, BIC shows the highest trends of 0.36 and 0.15 °C/decade, respectively. As for mean severity, NWA shows the highest trend of 0.06 per decade.

4.3 Sensitivity to the period

In this subsection, we assess the impact of averaging annual metrics over the two periods 1982-2023 and 1987-2022, being the temporal extent of REP and MEDREA, respectively. It is important to note that the climatological baseline period remains unchanged. The resulting differences are mostly due to the balance between the addition of the MHW active year of 2023 and the addition of the years 1982-1986, having low MHW activity (**Fig. 5**). Firstly, both periods show the same order of magnitude of period-averages and trends of annual metrics (**Tab. 2**). However, total days, mean duration, and cumulative intensity show higher means

over 1982-2023 than over 1987-2022, reflecting the very long duration of MHWs in 2023. On the contrary, maximum and mean intensities and mean severity have slightly higher means over 1987-2022 than over 1982-2023. Finally, total days, mean duration, maximum and mean intensities and mean severity have higher trends over 1982-2023 than over 1987-2022. This result highlights the exceptional contribution of the most recent years to long-term statistics, consistent with reports of unprecedented MHW activity in the western Mediterranean during 2022–2023 (Juza et al., 2024; Marullo et al., 2023).

4.4 Model assessment

In this subsection, we compare the surface MHW metrics derived from satellite observations (REP) with those from the model (MEDREA at 1m depth)

to assess the model's capability to reproduce the observed MHWs at the surface before its use for the subsurface MHW analyses. MHWs derived from REP and MEDREA have similar region-averaged annual metrics means, STDs and trends (**Tab. 2**) and subregion-averaged annual metrics values (**Figs. 5, 7-8**), both considered for 1987-2023, corroborating the accuracy of the model to reproduce the main features of observed MHW. Though systematic differences emerge from **Table 2**, MEDREA exhibits underestimations of the intensity-related metrics (maximum and mean intensity) and overestimations of persistence-related metrics (mean duration and total days). Also, for most annual metrics, MEDREA has a higher temporal variability than REP, highlighted by the larger STDs reported across most annual metrics. Also, MEDREA-derived trends in **Table 2** are higher than REP-derived trends for every annual metric except for mean duration, for which MEDREA does not show a significant trend. Comparing subregion-averaged annual metrics of **Figures 5, 7 and 8**, it is clear that MEDREA strongly overestimates total days in 2020 (121 days compared to 57 days in REP).

Thus, at the surface, the model MEDREA is relatively in agreement with observations for MHWs metrics, and it will now be used for the analysis of MHWs metrics in the subsurface.

5. Subsurface MHWs (MEDREA)

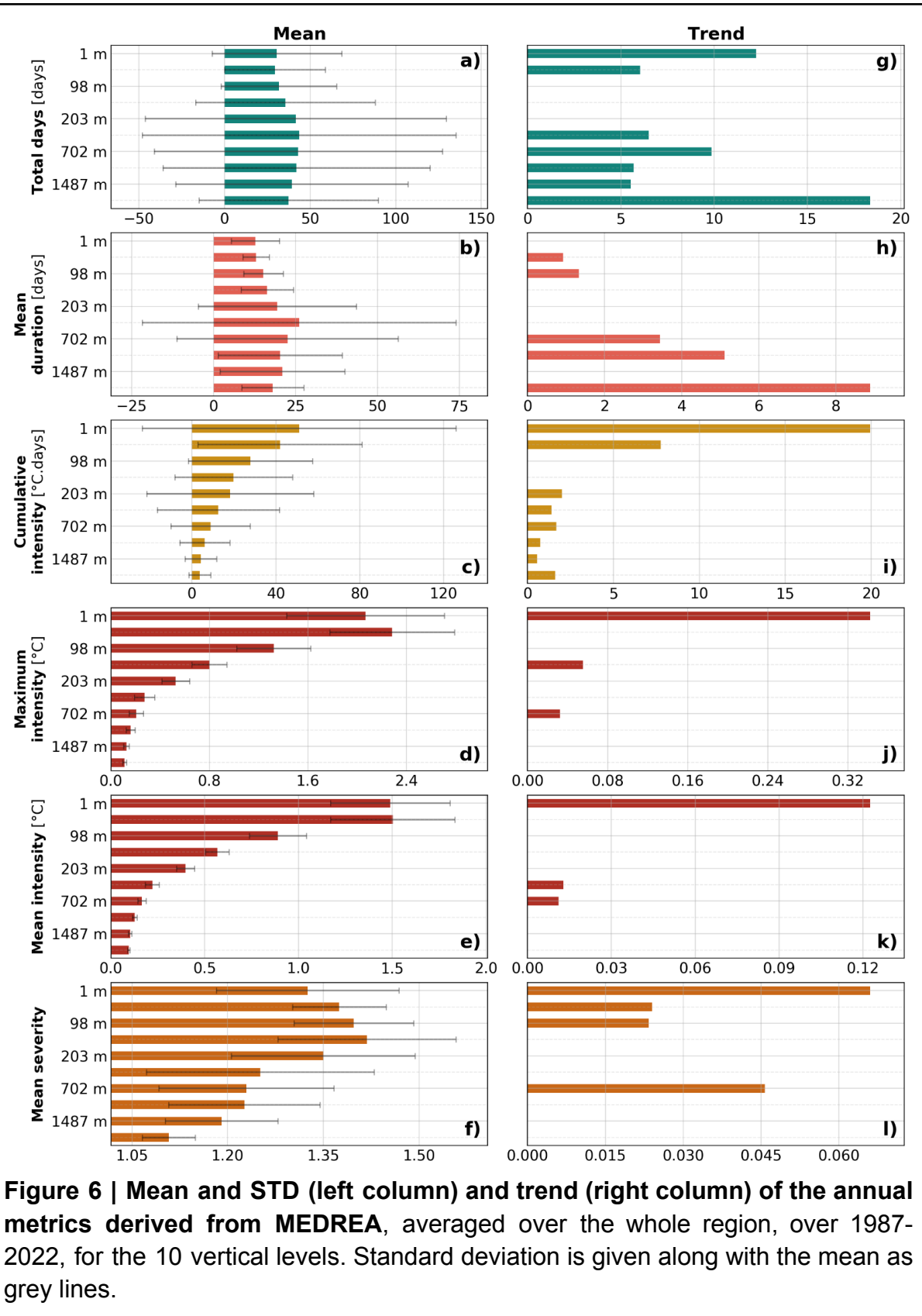
This section explores the temporal and spatial characteristics of MHWs at

various depths, revealing how these events manifest differently below the surface compared to the satellite-derived surface signals. The analysis of subsurface MHWs is conducted using the MEDREA model reanalysis data, which provides three-dimensional temperature fields and thus enables a systematic assessment of MHW persistence and intensity throughout the water column. By extending the study into the subsurface, we aim to capture processes that are not detectable from surface data alone (e.g. vertical propagation of thermal anomalies, depth-dependent variability in event persistence and intensity), and the distinct behaviour of coastal versus deeper regions.

In **Figure 6**, the mean and trends are calculated for different depths from annual MHW metrics averaged over the Balearic Islands region for the period 1987-2022. **Figures 7** and **8** show the evolution of annual metrics averaged in the four subregions for different depths over the same period, while **Figure 9** shows their associated statistics (means and trends), highlighting the variability at depth.

5.1. Regional analysis

In the Balearic Islands region, intensity-related metrics show their highest mean values at the surface and decrease with depth (**Fig. 6c-e**). Specifically, cumulative and mean intensities are strongest at the surface (51 °C·days and 1.49 °C, respectively), decreasing down to 4 °C·days and 0.09 °C, respectively (**Fig. 6c,e**). Maximum intensity also peaks near the surface, being highest at 51 m (2.28 °C),



decreasing down to 0.11 °C (Fig. 6d). Other annual metrics reach a maximum in the subsurface. Period-averaged total

days and mean duration peak at 493 m with values of 44 and 26.1 days, respectively, decreasing upwards until

31 and 12.7 days, respectively, and downwards until 37 and 18.0 days, respectively (**Fig. 6a-b**). Period-averaged mean severity shows a subsurface maximum at 153 m with a value of 1.42, with values decreasing upwards until 1.33 and downwards until 1.11 (**Fig. 6f**).

As shown in **Figure 6a-f**, the STD value for the total days, mean duration, and cumulative intensity annual metrics is high, relative to their mean value, highlighting a high temporal variability, as it has been noted at the surface in **Section 4.1**. For total days and mean duration, the STD reaches 92 and 47.9 days at 493 m, respectively, both being around twice their mean value at that depth (being 44 and 26.1 days, respectively) (**Fig. 6a-b**). At the surface, cumulative intensity shows a STD of 75 °C·days, being comparable to its mean value (51 °C·days). In contrast, for the maximum and mean intensity and mean severity, the STD is low compared to their mean values, highlighting lower temporal variability. Their maximum STDs are at 1 m, 51 m and 493 m, respectively, reaching 0.64 °C, 0.33 °C and 0.18, respectively (with mean values of 2.07 °C, 1.50°C and 1.25, respectively, at those depths). This difference in STD is also visible in the temporal evolution, the annual metrics present in **Figure 7** (total days, mean duration and cumulative intensity) showing very steep spikes, whereas the ones in **Figure 8** (maximum and mean intensity and mean severity) show less steep spikes.

The spikes exhibited by these time series correspond to specific MHW events that occurred in the Balearic Islands region. At 98 m, the 10 years with the highest region-averaged total

days are: 2020, 1990, 1998, 2017, 2016, 2019, 2008, 2021, 2018 and 2014, with values of 119, 110, 100, 91, 83, 68, 66, 63, 54 and 15 days, respectively (**Fig. 7iii**). The years presenting high values of total days are similar at the 51 and 98 m levels. Except for 2018, 2019 and 2021, all those years correspond to local maxima in the time series. At 1487 m, the 7 years with the highest total days are 2004, 2021, 2022, 2019, 2020, 2003 and 2005, with values of 218, 190, 187, 181, 176, 126 and 124 days, respectively (**Fig. 7ix**). This sequence is similar in the layers 1005 and 2001 m. During 2004, a high MHW activity was recorded from 702 to 2001 m (**Fig. 7vii-x**), with abnormal regional-averaged values at 1487 m of mean duration, cumulative, maximum and mean intensity and mean severity being of 63 days, 24 °C·days, 0.15 °C, 0.11 °C and 1.26, respectively. In recent years, high values of total days are observed, reaching subregion-averaged values over 300 days between 200 and 1500 m (**Fig. 7v-ix**). As illustrated in **Figure A3** (see Appendix 2), this near-perpetual MHW state can be explained by long-term sea warming. Indeed, as pointed out by Amaya et al. (2023b), using a fixed baseline as used herein, under ocean warming, MHW will grow more frequent and long-lasting until a ‘perpetual heatwave’ state is reached. This occurs when the temperature exceeds the 90th percentile climatology all year long. This particular aspect of the methodology will be open to perspectives in **Section 7**. Also, further investigation on specific subsurface MHW events will be conducted in **Sections 6.2 and 6.3**.

As shown in the previous section, MHW have become increasingly persis-

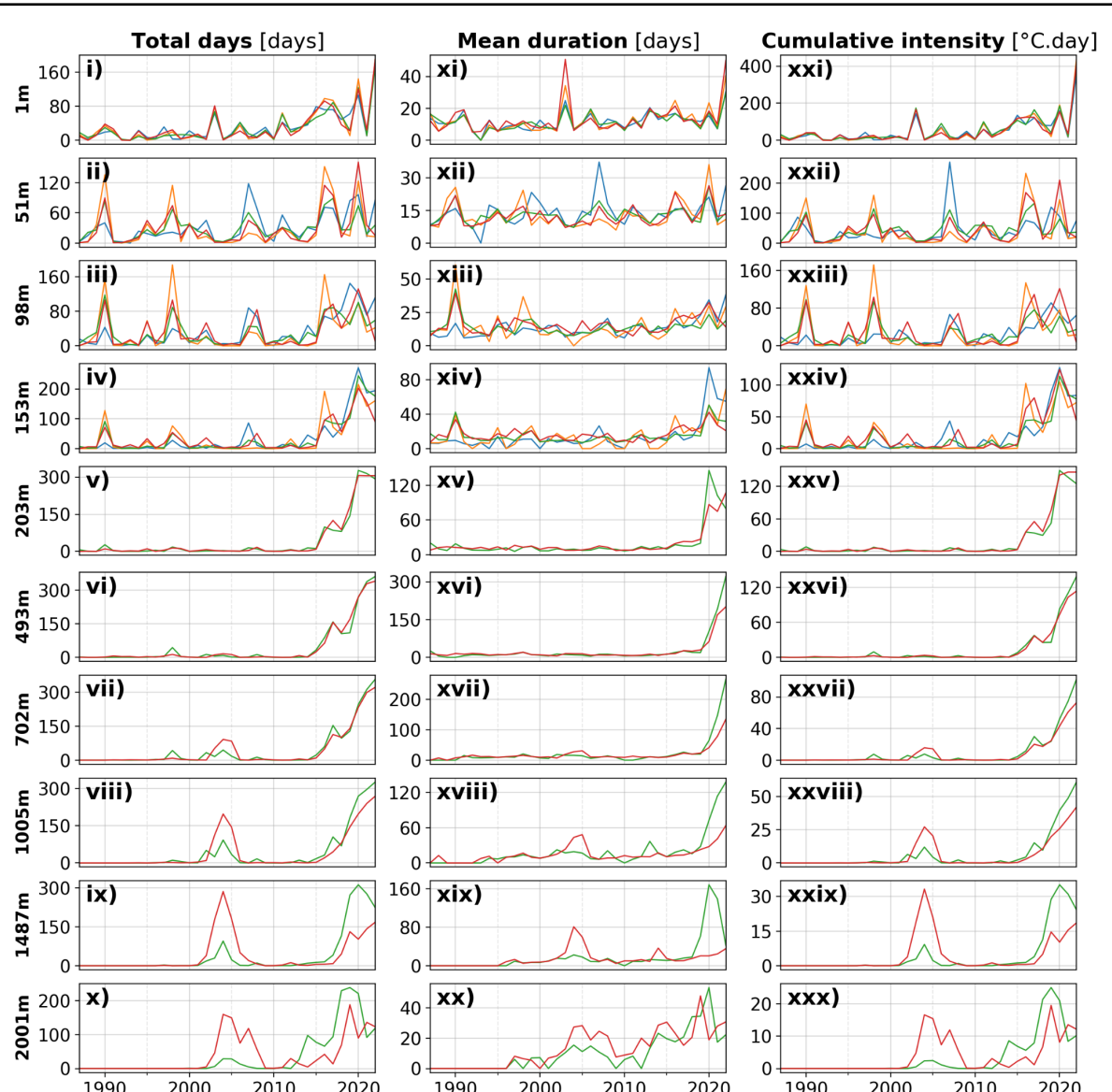


Figure 7 | Evolution of the total days, mean duration and cumulative intensity annual metrics derived from MEDREA, averaged over the four subregions, over 1987-2022, for the 10 vertical levels. Subregions are shown: SPC in blue, BIC in orange, BS in green and NWA in red.

tent and intense at the surface in the Balearic Islands region. A similar trend is perceptible below the surface. Indeed, as seen on **Figure 6g-l**, total days and cumulative intensity have more than 60% of analysed depth levels with significant positive trends (**Fig. 6g,i**). In contrast, mean duration, cumulative and mean intensity and mean severity show weaker signals, with only 30 to 50% of

the levels displaying significant increases (**Fig. 6h,j-l**). Importantly, these trends have values comparable to the mean value, with decadal trends ranging between one-half and one-tenth of their mean value, except for mean intensity and mean severity, which have lower trends. These results confirm that subsurface MHW activity follows the same strengthening tendency identified

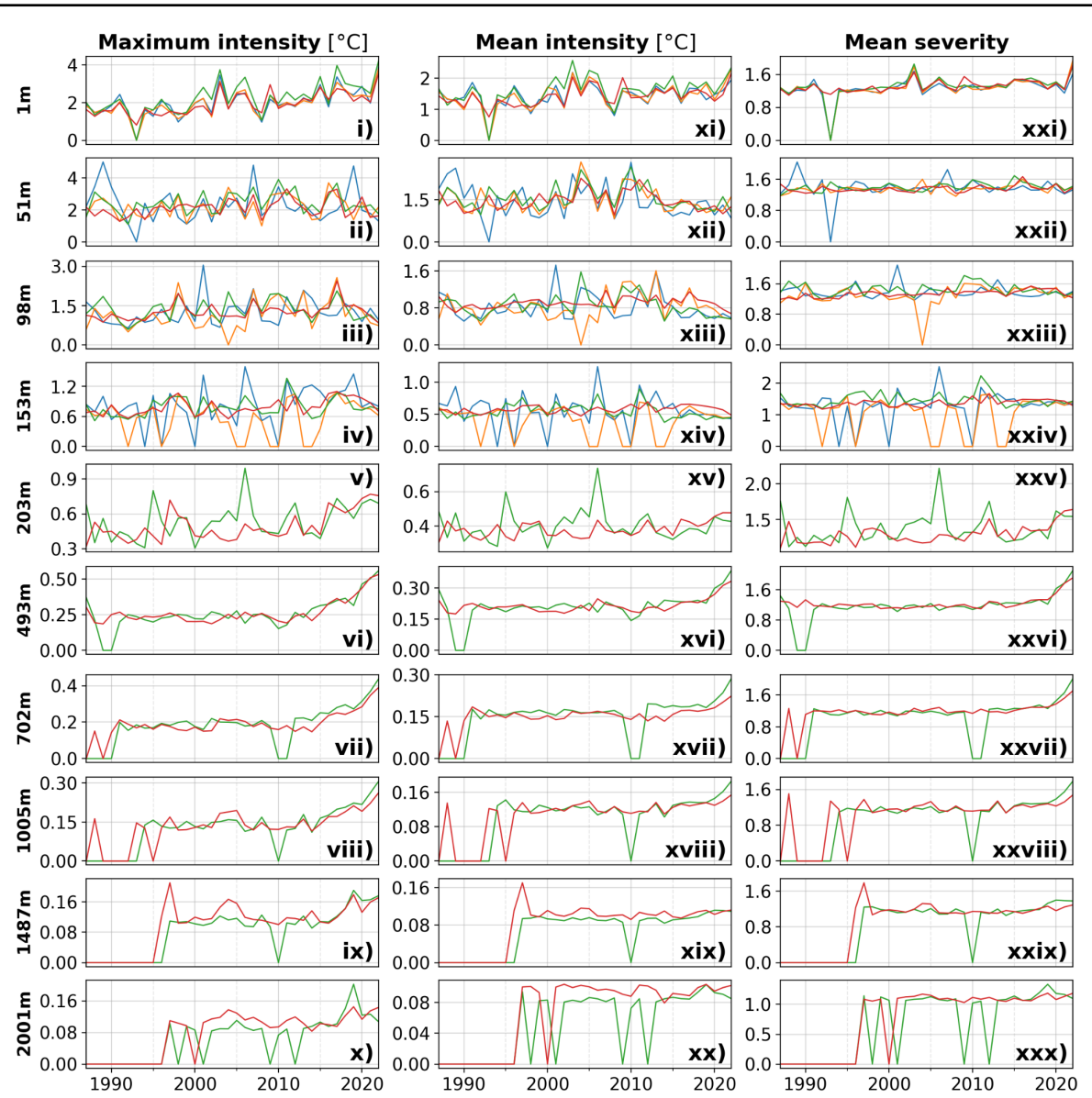


Figure 8 | Same as Figure 7 for maximum intensity, mean intensity and mean severity.

at the surface, though with marked variability across metrics and depth levels.

Over the water column, the distributions of these trends reveal clear differences among metrics (**Fig. 6g-l**). The trends of intensity-related and severity-related annual metrics have higher values at surface, decreasing progressively with depth. Specifically, the cumulative intensity trend decreases with depth from 19.9 down to 0.6

°C-days/decade, maximum intensity from 0.34 to 0.03 °C/decade, mean intensity from 0.12 to 0.01 °C/decade and mean severity from 0.07 to 0.02 per decade (**Fig. 6i-l**). In contrast, the mean duration trends increase with depth, rising from 0.92 at the surface to 8.89 days/decade at deeper levels (**Fig. 6h**). Concerning the total MHW days trend, the distribution is relatively uniform for the whole water column, with values ranging between 5 and 10 days/decade

except at the surface and at the bottom level (2001 m), with a stronger trend of 12.3 and 18.4 days/decade, respectively (**Fig. 6g**).

5.2. Subregional analysis

Figure 9 highlights subregional variability in means and trends for the period 1987-2022 over the water column. For a more succinct analysis, only half the levels considered in this study are shown. This selection is not expected to alter the findings of this subsection. Overall, the subregional variability is relatively low, with each subregion having similar mean and trend values for most metrics. As pointed out in the last section, among the four subregions, all annual metrics and depths, a meaningful fraction of the trends are significant and positive. Yet, among means and trends, differences can be noted between subregions.

Considering the first 200 meters, annual metrics are available in the four subregions. In that depth layer, total days show higher mean and trend values in SPC (**Fig. 9a,g**). For mean duration, the subregion showing the highest means and trends is BIC (**Fig. 9b,h**). SPC shows the highest trends of cumulative intensity, being significant in all levels in the first 200 m for this subregion (**Fig. 9i**). As for maximum and mean intensity, consistently with the study of the surface MHWs, BS show higher mean values (**Fig. 9d-e**), as well as for mean severity (**Fig. 9f**). Considering depths below 200 m, where values are only available in BS and NWA, mean and trend of duration are significantly higher in BS (**Fig. 9b,h**).

The same pattern is reflected in statistics of total days (being linked to mean duration), especially for trends, but also for the mean, being higher in BS (**Fig. 9a,g**). For maximum and mean intensity, means and trends are slightly higher in BS in general (**Fig. 9c-e,i-k**).

Overall, in the first 200 meters, coastal areas show slightly higher total days and duration. Also, BS shows high MHW activity, being more intense and severe in the first 200m than in the other subregions. Below 200 m, BS is also more persistent than NWA.

The study of MHWs in the region revealed marked variability at the subregional, vertical and temporal levels. This may reflect the wide range of complex drivers that can trigger MHW events.

6. Drivers of specific MHW events

The occurrence of surface and subsurface MHW events can be induced by various atmospheric and/or ocean processes (Capotondi et al., 2024; Zhang et al., 2023). Along this section, some MHW drivers will be explored in the Balearic Islands region.

6.1. Atmospheric forcing

The first driver that will be explored here is the main driver responsible for surface MHWs. It is characterised by enhanced air-sea heat fluxes and reduced wind-induced turbulent mixing, resulting in atmospheric-driven surface MHWs.

From the several extraordinary MHW intense years recorded at the surface in the Balearic Islands region

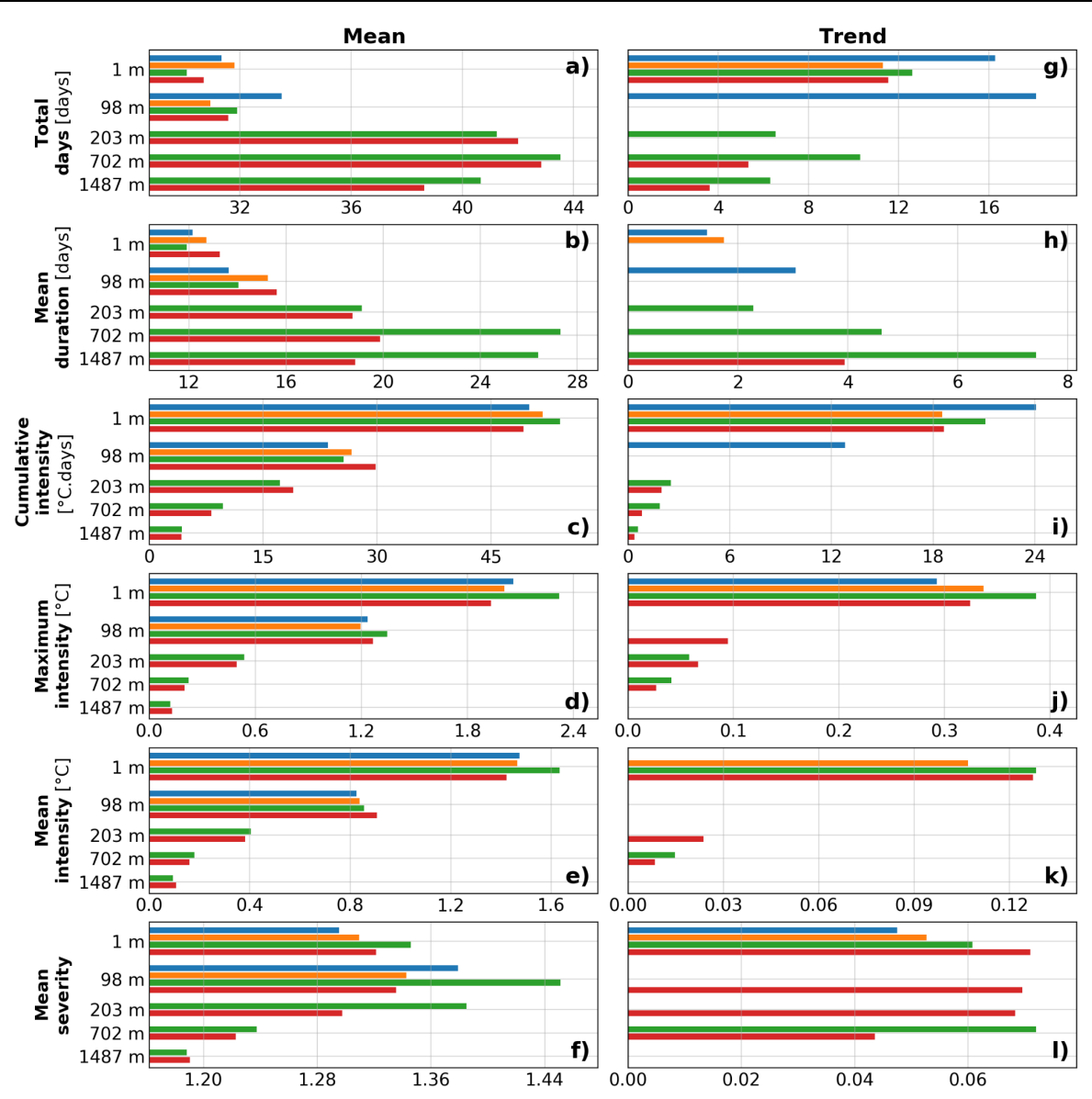


Figure 9 | Mean (left column) and trend (right column) of the total days, mean duration, cumulative, maximum and mean intensity and mean severity annual metrics derived from MEDREA, averaged over the four subregions, over 1987-2022, for the 10 vertical levels. Regions are shown: SPC in blue, BIC in orange, BS in green and NWA in red. Here, only BS and NWA are displayed below 200 m as SPC and BIC regions do not reach this depth.

mentioned in **Section 4.1**, 2003, 2022 and 2023 feature a common characteristic: they are associated with atmospheric heatwaves coupled with weak wind forcing. The 2003 event was the first basin-wide MHW recorded by satellites, having been widely studied and marked by unprecedented intensity

and persistence (Sparnocchia et al., 2006; Olita et al., 2007; Garrabou et al., 2009; Hobday et al., 2018; Holbrook et al., 2020; Martínez et al., 2023). 2022 has been the most MHW intense year recorded at the surface in the western Mediterranean at the time of writing (Juza et al., 2024; Estournel et al., 2025;

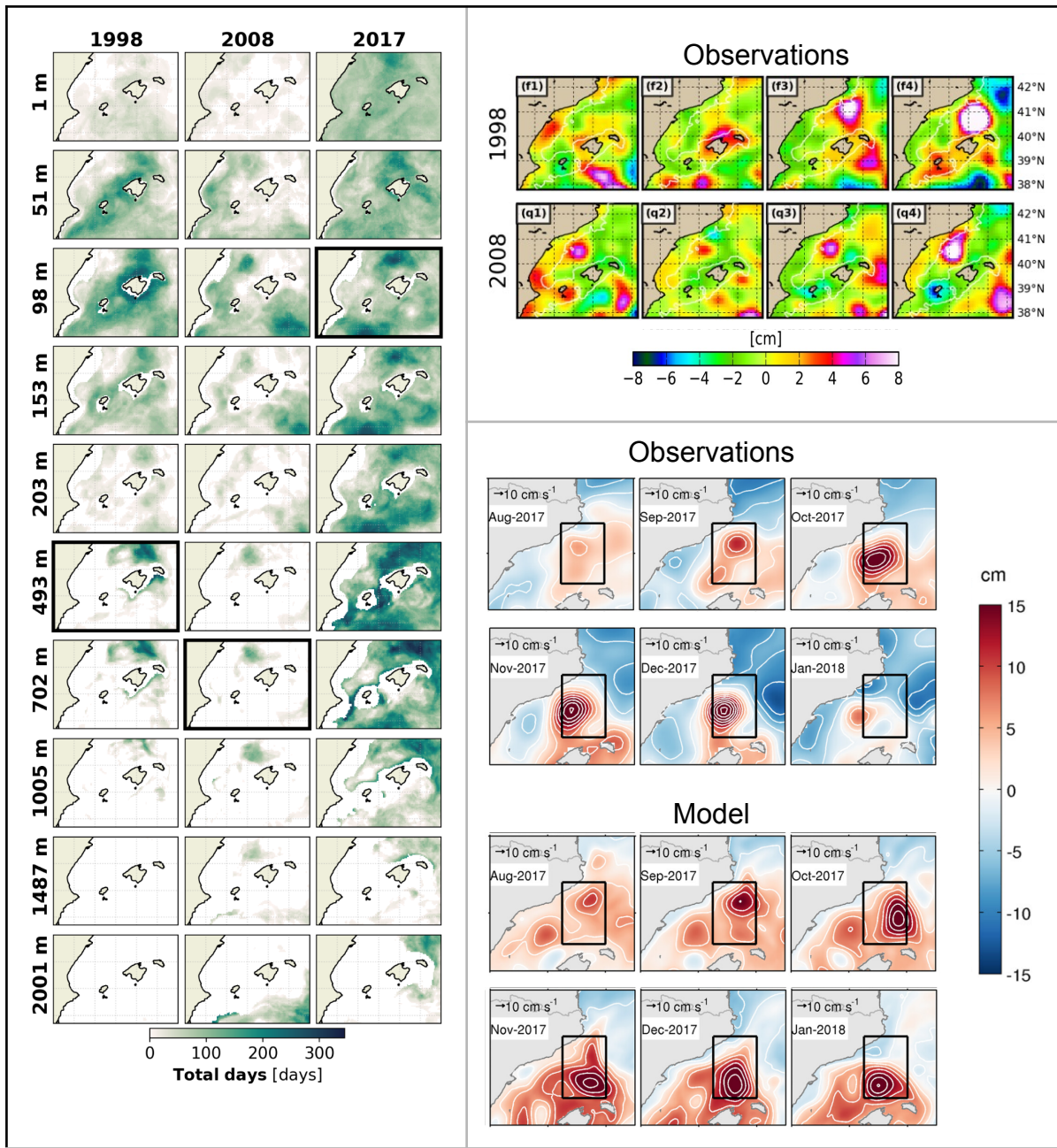


Figure 10 | Maps displaying the total days annual metric derived from MEDREA for the years 1998, 2008 and 2017 being influenced by anticyclonic eddies for the 10 vertical levels over the Balearic Islands region (left panel). Also, maps of SLA in 1998 and 2008 for the four seasons, from observations, from Mason and Pascual (2013) (upper right panel) and in 2017/2018, from observations and model, from Aguiar et al. (2022) (lower right panel). 1998, 2008 and 2017 eddies show the clearest signature at the 493, 1005 and 98 m level, respectively.

Marullo et al., 2023). 2023 has been the second warmest year on record for surface air temperature in Europe going back to 1850 (after 2020), according to the Copernicus Global Climate

Highlights (2023)³. As a consequence, exceptional SSTs were observed and

³ <https://climate.copernicus.eu/global-climate-highlights-2023>

associated with surface MHWs in the Mediterranean. For those three years, particular sea and atmosphere states resulted in significant surface MHWs.

However, low vertical mixing, due to high stratification and/or reduced wind-induced turbulent mixing, prevents the temperature anomaly from propagating to depth. Indeed, in 2003 and 2022, the exceptional surface MHWs do not show a signature in the annual metrics at depth (**Fig. 8**). The origin of subsurface MHWs comes from other drivers.

6.2. Anticyclonic eddies

Ocean heat advection and mixing are the main drivers of subsurface MHWs. Mesoscale eddies can be responsible for those processes. Specifically, anticyclonic eddies have a downwelling effect, propagating warm surface waters into colder deeper layers of the water column, which can result in subsurface MHWs.

Among the significant MHW intense years at the subsurface, 1998, 2008 and 2017 are of particular interest. Indeed, these years appear related to mesoscale eddy activity. This conclusion is reached by analysing **Figure 10**, where distinctive spatial anomalies in the total days annual metric emerge. These maps reveal localised maxima that propagate over the water column, aligned with mesoscale structures. After further investigation, these patterns are consistent with previous studies exhibiting anticyclonic eddies through sea level anomaly maps (for 1998 and 2008, Mason and Pascual, 2013; and for 2017, Aguiar et al., 2022). The spikes

shown for these three years have a signature in the time series of total days until 1005 m (**Fig. 7ii-viii**).

6.3. Other vertical processes

Other vertical ocean processes are responsible for subsurface MHWs such as convection and downwelling (Juza et al., 2022; Zhang et al., 2023; Capotondi et al., 2024). Those processes occur in the northwestern Mediterranean. Intermediate and deep convection occur during winter in the Gulf of Lion, located in the north of the Balearic Sea (Trestor et al., 2018). Also, according to Bakun and Agostini (2001), convergent ocean surface transport and downwelling can occur in the Balearic Sea due to its favourable wind pattern. These vertical processes mix upper warm waters with deeper cool waters, resulting in anomalously warm water at depth (Chevillard et al., 2024; Houpert et al., 2016).

Those processes could be related to the deep water events (700-2000 m) that have been identified in **Section 5.1** around the year 2004 and in recent years (since 2020 mostly). However, further studies would be required to identify the exact origin of those MHW events.

7. Conclusion and perspectives

In this study, satellite and model data enabled the analysis of MHWs at both surface and subsurface in the Balearic Islands region over the periods 1982-2023 and 1987-2022, respectively.

The analysis of the trends highlighted an increase in annual MHW metrics, at surface and subsurface, characterised by significant positive trends for a meaningful fraction of the metrics, subregions and depth levels. Concerning subregional variability, similar magnitudes in annual MHW metrics have been found in the four subregions over the water column, yet with some differences. At the surface, a north–south contrast stands out in MHW characteristics: northern subregions (CC, DBS) are dominated by stronger thermal intensities, while southern areas (BIC, DWAR) are more prone to longer-lasting events. This pattern changes with depth, as there is a high variability in the subregion dominance of MHW metrics. Below 200 m, BS displays more persistent, longer-lasting, and more intense MHWs with a higher mean severity than NWA. Regarding the vertical variability, intensity-related metrics (cumulative, maximum and mean intensity) are most pronounced at the surface and weaken with depth, whereas persistence-related metrics (mean duration and total days) reveal stronger signals in the intermediate layers (around 500 m). This vertical contrast suggests that while surface waters are most affected by the intensity of MHWs, deeper layers are more exposed to prolonged anomalous warming. The trends in annual metrics reveal a similar pattern, with a surface-dominated intensity signal and a subsurface-dominated persistence signal. Moreover, a high temporal variability in annual metrics was observed, particularly at the surface, fostering extraordinarily intense MHW years. Specific years have been

particularly investigated, as well as the drivers such as atmospheric forcing, mesoscale eddies, deep convection and downwelling processes that may have triggered their MHW activity.

Globally, the increase in MHW is primarily due to global warming (Oliver et al., 2018, 2019). In this regard, it has been proposed to consider approaches that account for long-term ocean warming during MHW calculations, such as the use of a shifting baseline (Amaya et al., 2023b). Whilst it was decided to consider a fixed baseline herein, following Hobday et al. (2016), it would be interesting to compare results with studies done with other baseline choices.

Finally, the outlined strong spatial and temporal variability described here suggests the need for sustained and continuous three-dimensional ocean monitoring to improve the detection and prediction of MHWs, from coastal to open ocean, from surface to deep waters. The code developed herein are written in an open-source programming language (Python) and are freely available (<https://github.com/arthur-gonnet/balearic-mhws-study>). They are intended to be modular in structure so that they can be implemented in operational systems. This work contributes in particular to the development and implementation of the regional DTO in the Balearic Sea by SOCIB. To take the study further, MHWs detection could be coupled with the study of biogeochemical (BGC) data in order to investigate the potential links existing between MHWs and BGC. Eventually, this study, firstly applied to the Balearic Islands region, could be extended to the whole Mediterranean,

while maintaining the subregional approach.

List of acronyms

SST	Sea Surface Temperature	MHW	Marine heatwave
REP	R EProcessed satellite-derived SST	MEDREA	M EDiterranean physical R EAnalysis
SPC	S panish P eninsular C oast	BIC	B alearic I slands C oast
BS	B alearic S ea	NWA	N orth- W estern A lgerian
STD	Standard deviation	SLA	Sea level anomaly

Data availability

All data used in this study are freely available on the Copernicus Marine Service platform (<https://marine.copernicus.eu/>).

REP: Mediterranean Sea - High Resolution L4 Sea Surface Temperature Reprocessed. *E.U. Copernicus Marine Service Information (CMEMS). Marine Data Store (MDS)*. doi: [10.48670/moi-00173](https://doi.org/10.48670/moi-00173) (Accessed on 5 Aug 2025).

MEDREA: Mediterranean Sea Physics Reanalysis. *E.U. Copernicus Marine Service Information (CMEMS). Marine Data Store (MDS)*. doi: [10.25423/CMCC/MEDSEA](https://doi.org/10.25423/CMCC/MEDSEA) [MULTIYEAR PHY 006 004 E3R1](https://doi.org/10.25423/CMCC/MEDSEA) (Accessed on 5 Aug 2025).

Code availability

All analyses were performed using Python. The original MHW detection code was written by Eric C.J. Oliver and is available through <https://github.com/ecjoliver/marineHeatWaves>. The source code used for the analysis in this paper

is publicly available on the GitHub repository at <https://github.com/arthur-gonnet/balearic-mhws-study>. Please note that the repository is not in its final state at the time of writing. Modifications for enhancing the code readability are planned after the release of this report. For trend calculations, the Python module *pyMannKendall* was used (see <https://github.com/mmhs013/pyMannKendall>).

References

- Aguiar, E., Mourre, B., Alvera-Azcárate, A., Pascual, A., Mason, E., & Tintoré, J. (2022). Strong Long-Lived Anticyclonic Mesoscale Eddies in the Balearic Sea: Formation, Intensification, and Thermal Impact. *J. Geophys. Res.: Oceans*, 127(5), e2021JC017589. doi: [10.1029/2021JC017589](https://doi.org/10.1029/2021JC017589)
- Amaya, D. J., Jacox, M. G., Alexander, M. A., Scott, J. D., Deser, C., Capotondi, A., & Phillips, A. S. (2023a). Bottom marine heatwaves along the continental shelves of North America. *Nat. Commun.*, 14(1), 1038. doi: [10.1038/s41467-023-36567-0](https://doi.org/10.1038/s41467-023-36567-0)

- Amaya, D. J., Jacox, M. G., Fewings, M. R., Saba, V. S., Stuecker, M. F., Rykaczewski, R. R. et al. (2023b). Marine heatwaves need clear definitions so coastal communities can adapt. *Nature*, 616(7955), 29–32. doi: [10.1038/d41586-023-00924-2](https://doi.org/10.1038/d41586-023-00924-2)
- Bakun, A., & Agostini, V. N. (2001). Seasonal patterns of wind-induced upwelling/downwelling in the Mediterranean Sea. *Sci. Mar.*, 65(3), 243–257. doi: [10.3989/scimar.2001.65n3243](https://doi.org/10.3989/scimar.2001.65n3243)
- Capotondi, A., Rodrigues, R. R., Sen Gupta, A., Benthuysen, J. A., Deser, C., Frölicher, T. L. et al. (2024). A global overview of marine heatwaves in a changing climate. *Commun. Earth Environ.*, 5(1), 701. doi: [10.1038/s43247-024-01806-9](https://doi.org/10.1038/s43247-024-01806-9)
- Cardona, L., Amigó, N., Ouled-Cheikh, J., Gazo, M., & Chicote, C. A. (2025). Cetaceans and sea turtles in the northern region of the Mediterranean Cetacean Migration Corridor: Abundance and multi-model habitat suitability analysis. *Front. Mar. Sci.*, 12, 1496039. doi: [10.3389/fmars.2025.1496039](https://doi.org/10.3389/fmars.2025.1496039)
- Cheng, L., Von Schuckmann, K., Minière, A., Hakuba, M. Z., Purkey, S., Schmidt, G. A., & Pan, Y. (2024). Ocean heat content in 2023. *Nat. Rev. Earth Environ.*, 5(4), 232–234. Doi: [10.1038/s43017-024-00539-9](https://doi.org/10.1038/s43017-024-00539-9)
- Chevillard, C., Juza, M., Díaz-Barroso, L., Reyes, E., Escudier, R., & Tintoré, J. (2024). Capability of the Mediterranean Argo network to monitor sub-regional climate change indicators. *Front. Mar. Sci.*, 11, 1416486. doi: [10.3389/fmars.2024.1416486](https://doi.org/10.3389/fmars.2024.1416486)
- Coll, M., Piroddi, C., Steenbeek, J., Kaschner, K., Ben Rais Lasram, F., Aguzzi, J. et al. (2010). The Biodiversity of the Mediterranean Sea: Estimates, Patterns, and Threats. *PLoS ONE*, 5(8), e111842. doi: [10.1371/journal.pone.00111842](https://doi.org/10.1371/journal.pone.00111842)
- Dayan, H., McAdam, R., Juza, M., Masina, S., & Speich, S. (2023). Marine heat waves in the Mediterranean Sea: An assessment from the surface to the subsurface to meet national needs. *Front. Mar. Sci.*, 10, 1045138. doi: [10.3389/fmars.2023.1045138](https://doi.org/10.3389/fmars.2023.1045138)
- Embry, O., Merchant, C. J., Good, S. A., Rayner, N. A., Høyer, J. L., Atkinson et al. (2024). Satellite-based time-series of sea-surface temperature since 1980 for climate applications. *Sci. Data*, 11(1), 326. doi: [10.1038/s41597-024-03147-w](https://doi.org/10.1038/s41597-024-03147-w)
- Escudier, R., Clementi, E., Omar, M., Cipollone, A., Pistoia, J., Aydogdu, A. et al. (2020). *Mediterranean Sea Physical Reanalysis (CMEMS MED-Currents, E3R1 system): MEDSEA_MULTIYEAR_PHY_006_004* (Version 1) [Data set]. Copernicus Monitoring Environment Marine Service (CMEMS). doi: [10.25423/CMCC/MEDSEA_MULTIYEAR_PHY_006_004_E3R1](https://doi.org/10.25423/CMCC/MEDSEA_MULTIYEAR_PHY_006_004_E3R1)
- Estournel, C., Estaqué, T., Ulles, C., Barral, Q.-B., & Marsaleix, P. (2025). Extreme sensitivity of the northeastern Gulf of Lion (western Mediterranean) to subsurface heatwaves: Physical processes and insights into effects on gorgonian populations in the summer of 2022. *Ocean Sci.*, 21(4), 1487–1503. doi: [10.5194/os-21-1487-2025](https://doi.org/10.5194/os-21-1487-2025)
- Fernández-Álvarez, B., Barceló-Llull, B., & Pascual, A. (2025). *Tracking Marine Heatwaves in the Balearic Sea: Temperature Trends and the Role of Detection Methods*. Remote Sensing/Climate and modes of variability. doi: [10.5194/egusphere-2024-4065](https://doi.org/10.5194/egusphere-2024-4065)
- Fernández-Barba, M., Huertas, I. E., & Navarro, G. (2024). Assessment of surface and bottom marine

- heatwaves along the Spanish coast. *Ocean Model.*, 190, 102399. doi: [10.1016/j.ocemod.2024.102399](https://doi.org/10.1016/j.ocemod.2024.102399)
- Frölicher, T. L., Fischer, E. M., & Gruber, N. (2018). Marine heatwaves under global warming. *Nature*, 560(7718), 360–364. doi: [10.1038/s41586-018-0383-9](https://doi.org/10.1038/s41586-018-0383-9)
- Garrabou, J., Coma, R., Bensoussan, N., Bally, M., Chevaldonné, P., Cigliano, M. et al. (2009). Mass mortality in Northwestern Mediterranean rocky benthic communities: Effects of the 2003 heat wave. *Glob. Change Biol.*, 15(5), 1090–1103. doi: [10.1111/j.1365-2486.2008.01823.x](https://doi.org/10.1111/j.1365-2486.2008.01823.x)
- Garrabou, J., Gómez-Gras, D., Medrano, A., Cerrano, C., Ponti, M., Schlegel, R. et al. (2022). Marine heatwaves drive recurrent mass mortalities in the Mediterranean Sea. *Glob. Change Biol.*, 28(19), 5708–5725. doi: [10.1111/gcb.16301](https://doi.org/10.1111/gcb.16301)
- Giorgi, F. (2006). Climate change hot-spots. *Geophys. Res. Lett.*, 33(8), 2006GL025734. doi: [10.1029/2006GL025734](https://doi.org/10.1029/2006GL025734)
- Guerrero-Meseguer, L., Marín, A., & Sanz-Lázaro, C. (2017). Future heat waves due to climate change threaten the survival of Posidonia oceanica seedlings. *Environ. Pollut.*, 230, 40–45. doi: [10.1016/j.envpol.2017.06.039](https://doi.org/10.1016/j.envpol.2017.06.039)
- Hamed, K. H., & Ramachandra Rao, A. (1998). A modified Mann-Kendall trend test for autocorrelated data. *J. Hydrol.*, 204(1–4), 182–196. doi: [10.1016/S0022-1694\(97\)00125-X](https://doi.org/10.1016/S0022-1694(97)00125-X)
- Helsel, D. R., Hirsch, R. M., Ryberg, K. R., Archfield, S. A., & Gilroy, G. (2020). *Statistical Methods in Water Resources* [Techniques and Methods] [Techniques and Methods].
- Hobday, A. J., Alexander, L. V., Perkins, S. E., Smale, D. A., Straub, S. C., Oliver, E. C. J. et al. (2016). A hierarchical approach to defining marine heatwaves. *Prog. Oceanogr.*, 141, 227–238. doi: [10.1016/j.pocean.2015.12.014](https://doi.org/10.1016/j.pocean.2015.12.014)
- Hobday, A., Oliver, E., Sen Gupta, A., Benthuysen, J., Burrows, M., Donat, M. et al. (2018). Categorizing and Naming Marine Heatwaves. *Oceanography*, 31(2). doi: [10.5670/oceanog.2018.205](https://doi.org/10.5670/oceanog.2018.205)
- Holbrook, N. J., Scannell, H. A., Sen Gupta, A., Benthuysen, J. A., Feng, M., Oliver, E. C. J. et al. (2019). A global assessment of marine heatwaves and their drivers. *Nat. Commun.*, 10(1), 2624. doi: [10.1038/s41467-019-10206-z](https://doi.org/10.1038/s41467-019-10206-z)
- Holbrook, N. J., Sen Gupta, A., Oliver, E. C. J., Hobday, A. J., Benthuysen, J. A., Scannell, H. et al. (2020). Keeping pace with marine heatwaves. *Nat. Rev. Earth Environ.*, 1(9), 482–493. doi: [10.1038/s43017-020-0068-4](https://doi.org/10.1038/s43017-020-0068-4)
- Houpert, L., Durrieu De Madron, X., Testor, P., Bosse, A., D'Ortenzio, F., Bouin, M. N. et al. (2016). Observations of open-ocean deep convection in the northwestern Mediterranean Sea: Seasonal and interannual variability of mixing and deep water masses for the 2007–2013 Period: DEEP CONVECTION OBS. NW MED 2007–2013. *J. Geophys. Res.: Oceans*, 121(11), 8139–8171. doi: [10.1002/2016JC011857](https://doi.org/10.1002/2016JC011857)
- Juza, M., De Alfonso, M., & Fernández-Mora, Á. (2024). Coastal ocean response during the unprecedented marine heatwaves in the western Mediterranean in 2022. *State of the Planet*, 4-osr8, 1–11. doi: [10.5194/sp-4-osr8-14-2024](https://doi.org/10.5194/sp-4-osr8-14-2024)
- Juza, M., Fernández-Mora, Á., & Tintoré, J. (2022). Sub-Regional Marine Heat Waves in the Mediterranean Sea From Observations: Long-Term Surface Changes, Sub-Surface and Coastal Responses. *Front. Mar. Sci.*,

- 9, 785771. doi: [10.3389/fmars.2022.785771](https://doi.org/10.3389/fmars.2022.785771)
- Juza, M., & Tintoré, J. (2020). *Sub-regional Mediterranean Sea Indicators: From event detection to climate change* [Web app]. SOCIB. <https://apps.socib.es/subregmed-indicators>
- Juza, M., & Tintoré, J. (2021). Multivariate Sub-Regional Ocean Indicators in the Mediterranean Sea: From Event Detection to Climate Change Estimations. *Front. Mar. Sci.*, 8, 610589. doi: [10.3389/fmars.2021.610589](https://doi.org/10.3389/fmars.2021.610589)
- Lavigne, H., D'Ortenzio, F., Ribera D'Alcalà, M., Claustre, H., Sauzède, R., & Gacic, M. (2015). On the vertical distribution of the chlorophyll *a* concentration in the Mediterranean Sea: A basin-scale and seasonal approach. *Biogeosciences*, 12(16), 5021–5039. doi: [10.5194/bg-12-5021-2015](https://doi.org/10.5194/bg-12-5021-2015)
- Levitus, S., Antonov, J., & Boyer, T. (2005). Warming of the world ocean, 1955–2003. *Geophys. Res. Lett.*, 32(2), 2004GL021592. doi: [10.1029/2004GL021592](https://doi.org/10.1029/2004GL021592)
- Lionello, P., & Scarascia, L. (2018). The relation between climate change in the Mediterranean region and global warming. *Reg. Environ. Change*, 18(5), 1481–1493. doi: [10.1007/s10113-018-1290-1](https://doi.org/10.1007/s10113-018-1290-1)
- Martínez, J., Leonelli, F. E., García-Ladona, E., Garrabou, J., Kersting, D. K., Bensoussan, N., & Pisano, A. (2023). Evolution of marine heatwaves in warming seas: The Mediterranean Sea case study. *Front. Mar. Sci.*, 10, 1193164. doi: [10.3389/fmars.2023.1193164](https://doi.org/10.3389/fmars.2023.1193164)
- Marullo, S., Serva, F., Iacono, R., Napolitano, E., Di Sarra, A., Meloni, D. et al. (2023). Record-breaking persistence of the 2022/23 marine heatwave in the Mediterranean Sea. *Environ. Res. Lett.*, 18(11), 114041. doi: [10.1088/1748-9326/ad02ae](https://doi.org/10.1088/1748-9326/ad02ae)
- Mason, E., & Pascual, A. (2013). Multiscale variability in the Balearic Sea: An altimetric perspective. *J. Geophys. Res.: Oceans*, 118(6), 3007–3025. doi: [10.1002/jgrc.20234](https://doi.org/10.1002/jgrc.20234)
- Millot, C. (1999). Circulation in the Western Mediterranean Sea. *J. Mar. Syst.*, 20(1–4), 423–442. doi: [10.1016/S0924-7963\(98\)00078-5](https://doi.org/10.1016/S0924-7963(98)00078-5)
- Mitchell, J. F. B., Lowe, J., Wood, R. A., & Vellinga, M. (2006). Extreme events due to human-induced climate change. *Philos. Trans. R. Soc. A*, 364(1845), 2117–2133. doi: [10.1098/rsta.2006.1816](https://doi.org/10.1098/rsta.2006.1816)
- Olita, A., Sorgente, R., Natale, S., Gaberšek, S., Ribotti, A., Bonanno, A., & Patti, B. (2007). Effects of the 2003 European heatwave on the Central Mediterranean Sea: Surface fluxes and the dynamical response. *Ocean Sci.*, 3(2), 273–289. doi: [10.5194/os-3-273-2007](https://doi.org/10.5194/os-3-273-2007)
- Oliver, E. C. J. (2019). Mean warming not variability drives marine heatwave trends. *Clim. Dyn.*, 53(3–4), 1653–1659. doi: [10.1007/s00382-019-04707-2](https://doi.org/10.1007/s00382-019-04707-2)
- Oliver, E. C. J., Donat, M. G., Burrows, M. T., Moore, P. J., Smale, D. A., Alexander, L. V. et al. (2018). Longer and more frequent marine heatwaves over the past century. *Nat. Commun.*, 9(1), 1324. doi: [10.1038/s41467-018-03732-9](https://doi.org/10.1038/s41467-018-03732-9)
- Pan, Y., Minière, A., Von Schuckmann, K., Li, Z., Li, Y., Cheng, L., & Zhu, J. (2025). Ocean heat content in 2024. *Nat. Rev. Earth Environ.*, 6(4), 249–251. doi: [10.1038/s43017-025-00655-0](https://doi.org/10.1038/s43017-025-00655-0)
- Pastor, F., & Khodayar, S. (2023). Marine heat waves: Characterizing a major climate impact in the Mediterranean. *Sci. Total Environ.*, 861, 160621. doi: [10.1016/j.scitotenv.2022.160621](https://doi.org/10.1016/j.scitotenv.2022.160621)
- Pinot, J.-M., Tintoré, J., & Gomis, D. (1995). Multivariate analysis of the surface circulation in the Balearic Sea. *Prog. Oceanogr.*, 36(4),

- 343–376. doi: [10.1016/0079-6611\(96\)00003-1](https://doi.org/10.1016/0079-6611(96)00003-1)
- Pisano, A., Buongiorno Nardelli, B., Tronconi, C., & Santoleri, R. (2016). The new Mediterranean optimally interpolated pathfinder AVHRR SST Dataset (1982–2012). *Remote Sens. Environ.*, 176, 107–116. doi: [10.1016/j.rse.2016.01.019](https://doi.org/10.1016/j.rse.2016.01.019)
- Pisano, A., Marullo, S., Artale, V., Falcini, F., Yang, C., Leonelli, F. E. et al. (2020). New Evidence of Mediterranean Climate Change and Variability from Sea Surface Temperature Observations. *Remote Sens.*, 12(1), 132. doi: [10.3390/rs12010132](https://doi.org/10.3390/rs12010132)
- Reyes, E., Charcos-Llorens, M., Fernández-Mora, À., Gómez, A. G., Révelard, A., Juza, M. et al. (2024). *Co-design, Implementation and Management Plan of the Different Digital Twin Prototypes in the Balearic Sea [Plan]*. SOCIB. https://www.socib.es/media/uploads/productions/1410_en_3d48cbce0c663d801cd768ad667b2d3b521e2f6a.pdf
- Rosselló, P., Pascual, A., & Combes, V. (2023). Assessing marine heat waves in the Mediterranean Sea: A comparison of fixed and moving baseline methods. *Front. Mar. Sci.*, 10, 1168368. doi: [10.3389/fmars.2023.1168368](https://doi.org/10.3389/fmars.2023.1168368)
- Salat, J., Puig, P., & Latasa, M. (2010). Violent storms within the Sea: Dense water formation episodes in the NW Mediterranean. *Adv. Geosci.*, 26, 53–59. doi: [10.5194/adgeo-26-53-2010](https://doi.org/10.5194/adgeo-26-53-2010)
- Schaeffer, A., & Roughan, M. (2017). Subsurface intensification of marine heatwaves off southeastern Australia: The role of stratification and local winds. *Geophys. Res. Lett.*, 44(10), 5025–5033. doi: [10.1002/2017GL073714](https://doi.org/10.1002/2017GL073714)
- Sen Gupta, A., Thomsen, M., Benthuysen, J. A., Hobday, A. J., Oliver, E., Alexander, L. V. et al. (2020). Drivers and impacts of the most extreme marine heatwave events. *Sci. Rep.*, 10(1), 19359. doi: [10.1038/s41598-020-75445-3](https://doi.org/10.1038/s41598-020-75445-3)
- Simon, A., Pires, C., Frölicher, T. L., & Russo, A. (2023). Long-term warming and interannual variability contributions to marine heatwaves in the Mediterranean. *Weather Clim. Extremes*, 42, 100619. doi: [10.1016/j.wace.2023.100619](https://doi.org/10.1016/j.wace.2023.100619)
- Smith, K. E., Burrows, M. T., Hobday, A. J., Sen Gupta, A., Moore, P. J., Thomsen, M. et al. (2021). Socioeconomic impacts of marine heatwaves: Global issues and opportunities. *Science*, 374(6566), eabj3593. doi: [10.1126/science.abj3593](https://doi.org/10.1126/science.abj3593)
- Sparnocchia, S., Schiano, M. E., Picco, P., Bozzano, R., & Cappelletti, A. (2006). The anomalous warming of summer 2003 in the surface layer of the Central Ligurian Sea (Western Mediterranean). *Ann. Geophys.*, 24(2), 443–452. doi: [10.5194/angeo-24-443-2006](https://doi.org/10.5194/angeo-24-443-2006)
- Stipcich, P., Marín-Guirao, L., Pansini, A., Pinna, F., Procaccini, G., Pusceddu, A. et al. (2022). Effects of Current and Future Summer Marine Heat Waves on Posidonia oceanica: Plant Origin Matters? *Front. Clim.*, 4, 844831. doi: [10.3389/fclim.2022.844831](https://doi.org/10.3389/fclim.2022.844831)
- Testor, P., Bosse, A., Houpert, L., Margirier, F., Mortier, L., Legoff, H. et al. (2018). Multiscale Observations of Deep Convection in the Northwestern Mediterranean Sea During Winter 2012–2013 Using Multiple Platforms. *J. Geophys. Res.: Oceans*, 123(3), 1745–1776. doi: [10.1002/2016JC012671](https://doi.org/10.1002/2016JC012671)
- United Nations Environment Programme. (2021). *State of the Environment and Development in the Mediterranean (SoED) 2020*.

- United Nations. doi:
[10.18356/9789280737967](https://doi.org/10.18356/9789280737967)
- Von Schuckmann, K., Moreira, L., Grégoire, M., Marcos, M., Staneva, J., Brasseur, P. et al. (2024). *8th edition of the Copernicus Ocean State Report (OSR8)* (0 edn). Copernicus GmbH. doi:
[10.5194/sp-4-osr8](https://doi.org/10.5194/sp-4-osr8)
- Wang, F., Shao, W., Yu, H., Kan, G., He, X., Zhang, D., Ren, M., & Wang, G. (2020). Re-evaluation of the Power of the Mann-Kendall Test for Detecting Monotonic Trends in Hydrometeorological Time Series. *Front. Earth Sci.*, 8, 14. doi:
[10.3389/feart.2020.00014](https://doi.org/10.3389/feart.2020.00014)
- Wernberg, T., Smale, D. A., Tuya, F., Thomsen, M. S., Langlois, T. J., De Bettignies, T., Bennett, S., & Rousseaux, C. S. (2013). An extreme climatic event alters marine ecosystem structure in a global biodiversity hotspot. *Nat. Clim. Chang.*, 3(1), 78–82. doi:
[10.1038/nclimate1627](https://doi.org/10.1038/nclimate1627)
- Zhang, Y., Du, Y., Feng, M., & Hobday, A. J. (2023). Vertical structures of marine heatwaves. *Nat. Commun.*, 14(1), 6483. doi:
[10.1038/s41467-023-42219](https://doi.org/10.1038/s41467-023-42219)

Appendix 1: Global overview of total days and maximum intensity

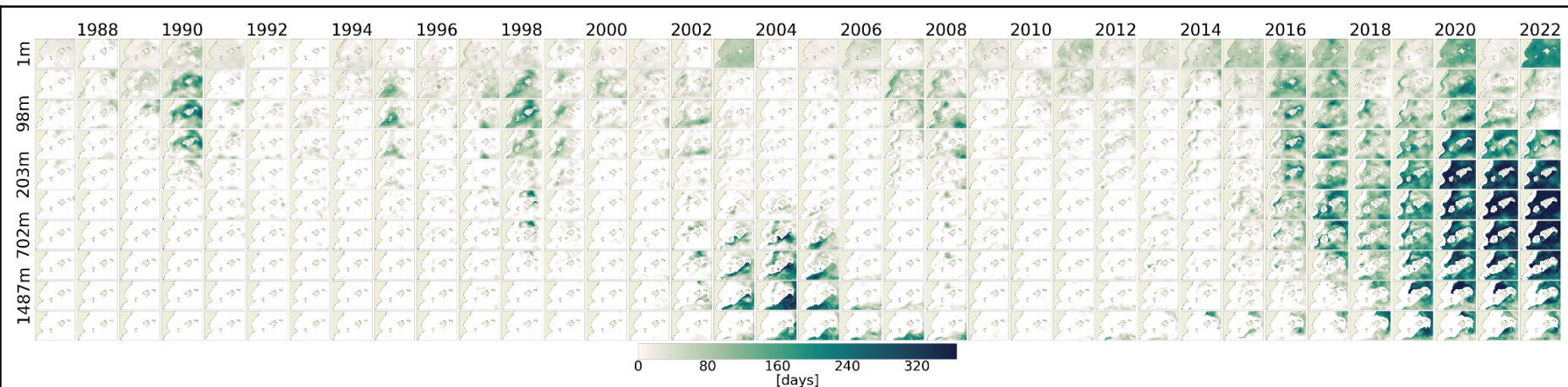


Figure A1 | Annual maps of total days derived from MEDREA, abscissa is the year (from 1987 to 2022), ordinate is the depth (from 1m to 2001m).

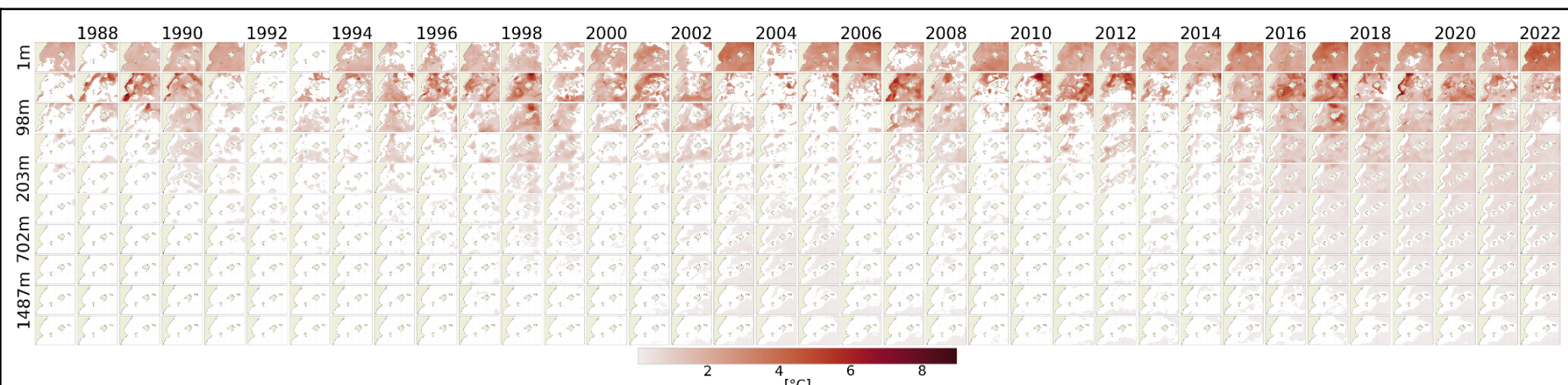


Figure A2 | Same as Figure A1 for maximum intensity.

Appendix 2: Time series of temperature

